

SENSORLESS DRIVE FOR HIGH-SPEED BLDC MOTORS USING SEPIC CONVERTER FOR PV APPLICATIONS

Dr.C.Rajselvan^[1], Ms.C.Ramya^[2] , Ms.A.Kaveri^[3],
Department of Electrical and Electronics Engineering
Dhanalakshmi Srinivasan College of Engineering and Technology

ABSTRACT

This project proposes a simple, cost effective and efficient brushless DC (BLDC) motor drive for solar photovoltaic (SPV) array system. A Sepic converter is utilized in order to extract the maximum available power from the SPV array. In order to improve the performance of the high-speed brushless direct current (BLDC) motor drives, a novel high-precision Sensorless drive has been developed. It is well known that, the inevitable voltage pulses, which are generated during the commutation periods, will impact the rotor position detecting accuracy, and further impact the performance of the overall sensorless drive, especially in the higher speed range or under the heavier load conditions. For this reason, the active compensation method based on the virtual 3rd harmonic back-EMF (the back electromotive force) incorporating the SFF- SOGI-PLL (synchronic-frequency filter incorporating the second-order generalized integrator based phase-locked loop) is proposed to precise detect the commutation points for sensorless drive.

Keywords: Solar photovoltaic system, SEPIC, BLDC, Sensorless

1. INTRODUCTION

In recent years, owing to the advantages of its compactness, maintenance, high efficiency and low cost, the brushless direct current (BLDC) motors are getting more and more attention in many areas like the blower and compressor, especially in the high- speed applications [1-3]. Commonly, the speed of the high-speed motor could reach up tens of thousands revolutions per minute (r/min) according to the bearing [4, 5]. Meanwhile, the load power of the motor developed for the blower type applications is increasing with the motor speed [6]. Therefore, precise detecting of the rotor position for the sensorless drive scheme is essential to ensure the high efficiency and low loss of the overall system, especially in the high-speed range. It is well known that, for the operation of the inverter in BLDC control system, six discrete rotor position signals in one rotating cycle are required. Conventionally, the rotor position detecting methods can be classified into two categories: the mechanical position sensor-based methods and the sensorless methods. The typical sensors include the resolver, the encoder [8] and the Hall-effect sensor [9], which is traditionally used in the mechanical position sensor-based methods. However, these mechanical sensors need special arrangements to be mounted as well as increasing the cost, which limits the application in the high-speed motors. Hence, more and more researches are focused on the sensorless-based methods. Numerous of sensorless-based methods have been reported in the pre-researches, which mainly contain the back-EMFs based method, the 3rd harmonic based method, the integration based

method, the phase-locked loop (PLL) based method, and the flux linkage estimation based method and the other sensorless method. Among the sensorless drive methods, the most popular category is the back-EMF based method.

The various sensors less control strategies are; the open phase current sensing method, the third harmonic of back-EMF detection method, the back-EMF detection method and the open phase voltage sensing method. All these methods do not provide a high performance at low speed ranges [3-6]. To solve this problem, a new sensor less control method utilizing an unknown input observer is used. The unknown input observer has been widely researched [7- 9], especially in the fault detection field [10-12]. However, this observer has not been adopted in sensor less BLDC motor control application. Hence, this paper presents a new sensor less control method incorporating an unknown input observer that is independent of the rotor speed for a BLDC motor drive. As a result, this paper proposes a highly useful new solution for a sensor less BLDC motor drive, which can effectively estimate a line-to-line back-EMF.

EXISTING METHODS

- Conventionally, the rotor position detecting methods can be classified into two categories: the mechanical position sensor-based methods and the sensorless methods.
- The typical sensors include the resolver the encoder and the Hall-effect sensor, which is traditionally, used in the mechanical position sensor-based methods.
- Phase-locked loop (PLL) based method.
- Kalman filter is used in a back-EMF integration based sensorless method for reluctance machines to smooth the noise.

PROPOSED SYSTEM

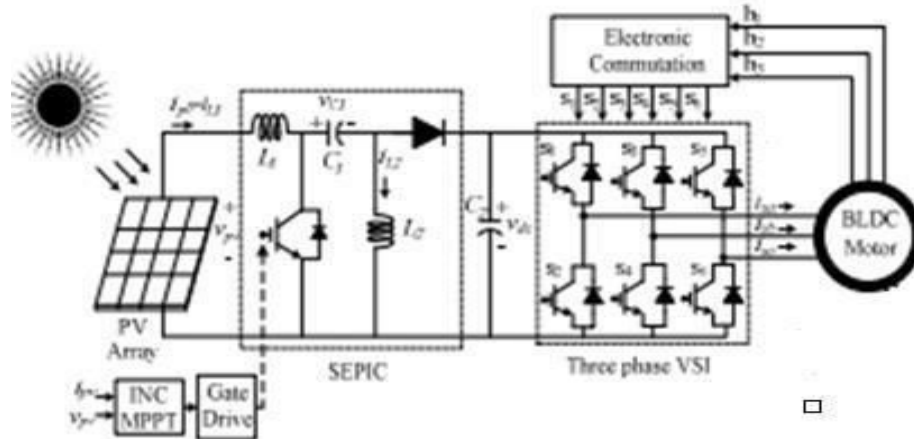
- A novel high-precision sensorless drive method for BLDC motors is proposed.
- The proposed method can compensate the commutation error adaptively in a wide operating range, and does not need the neutral wire at the mean time.
- A synchronic-frequency filter (SFF) is put up as a pre-filter to improve the performance of SOGI-PLL.

CONFIGURATION OF THE PROPOSED SYSTEM

The proposed system under study is shown in Fig. 4. The system consists of the SPV array followed by the SEPIC which feeds the VSI, supplying the BLDC motor coupled to a centrifugal type of water pump. MPPT algorithm generates switching pulse for the switch of SEPIC whereas the electronic

commutation generates the switching sequence for the switches of the VSI. The Back Emf signals provided by the encoder, mounted on the BLDC motor is logically converted into the 6 pulses for the 6

switches of the VSI. The design and control of each stage of the configuration shown in Fig. 4 are elaborated in the following sections.



SEPIC CONVERTER WITH PV AND MPPT

PV system directly converts sunlight into electricity. The basic device of a PV system is the PV cell. Cells may be gathered to form modules or arrays. More sophisticated applications require DC-DC converters to process the electricity from the PV device. These converters may be used to either increase or decrease the PV system voltage at the load. The proposed SEPIC converter operates in boost mode.

A. PV Module Characteristics

The practical equivalent circuit of a PV module is shown in fig.2 [2]., while the typical output characteristics are shown in fig.3

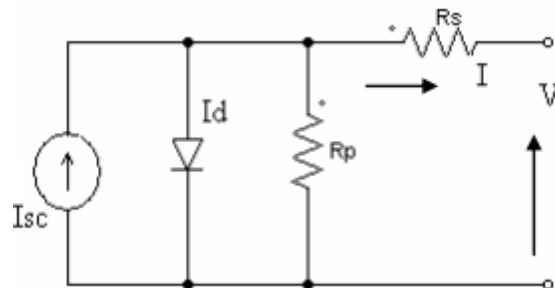


Fig. 2 Equivalent circuit of a PV module

In the equivalent circuit, the current source represents the current generated by light photons and its output is constant under constant temperature and constant irradiance. The diode shunted with the

current source determines the I-V characteristics of PV module. There is a series of resistance in a current path through the semiconductor material, the metal grid, contacts, and a current collecting bus. These

resistive losses are lumped together as a series resistor (R_s). Its effect becomes very noteworthy in a PV module. The loss associated with a small leakage of current through a resistive path in parallel with the intrinsic device is represented by a parallel resistor (R_p). Its effect is much less noteworthy in a PV module compared to the series resistance, and it will only become noticeable when a number of PV modules are connected in parallel for a larger system. The characteristic equation which represents the I-V characteristic of a practical photovoltaic module is given below

$$I = I_{pv} - I_o \left[\exp\left(\frac{V + IR_s}{V_{tn}}\right) - 1 \right] - \frac{V + IR_s}{R_p}$$

Where I and V are the PV cell current and voltage respectively, I_{pv} is the photovoltaic current, I_o is the reverse saturation current of diode, $V_t = N_s k T / q$ is the thermal voltage of the array with N_s cells connected in series, k is the Boltzmann constant ($1.3806 \times 10^{-23} \text{ J/K}$), T is the temperature of the p-n junction, q is the electron charge and n is the diode ideality constant. I_{pv} and I_o are given as follows [9]

$$I_{pv} = \left\{ \left[1 + a(T - T_{ref}) \right] I_{sc} \right\} \left[\frac{G}{1000} \right]$$

$$I_o = I_o(T_{ref}) \left[\frac{T}{T_{ref}} \right]^{\frac{3}{n}} e^{-\frac{qE_g}{nk} \left[\frac{1}{T_{ref}} - \frac{1}{T} \right]}$$

Where “ a ” is temperature coefficient of I_{sc} , G is the given irradiance in W/m^2 and E_g is the band gap energy (1.16 eV for Si). The single PV module specification is given in table I.

TABLE I PV MODULE BPSX150S SPECIFICATIONS

Electrical Characteristics	Value
Maximum Power (P_{max})	150W
Voltage at P_{max} (V_{mp})	34.5V
Current at P_{max} (I_{mp})	4.35A
Open-circuit voltage (V_{oc})	43.5V
Short-circuit current (I_{sc})	4.75A
Temperature coefficient of I_{sc}	$0.065 \pm 0.015\% / ^\circ\text{C}$
Temperature coefficient of V_{oc}	$-160 \pm 20 \text{ mV} / ^\circ\text{C}$

Fig. 3 PV Module IV and PV characteristics

B.MPPT Control Algorithm

There are various types of maximum power point tracking algorithms available. Among them, P&O algorithm is used here, since it has the advantages of high tracking efficiency, low cost, easy implementation etc. In this algorithm a slight perturbation is introduced in the system voltage. Due to this perturbation, the power of the module changes [8]. If the power increases due to the perturbation then the next perturbation is continued in the same direction. After the peak power is reached the power at the next instant decreases and hence after that the direction of perturbation reverses. When the steady state is reached the algorithm oscillates around the peak point [8]. In order to keep the power variation small the perturbation size is kept very small. The algorithm is developed in such a manner that it sets a reference voltage of the module corresponding to the peak voltage of the module.

C.Modeling of SEPIC Converter

The important requirement of any DC–DC converter used in the MPPT scheme is that it should have a low input current ripple. Buck converters will produce ripples on the PV module side currents and thus require a larger value of input capacitance on the module side. On the other hand, boost converters will present low ripple on the PV module side, but the load current exhibits more ripple and gives a voltage higher than the array. Furthermore, the load voltage will be inverted with buck–boost or CUK converters. Under these conditions, the SEPIC converter, provide the buck–boost conversion function without polarity reversal, in addition to the low ripple current on the source and load sides. The SEPIC (Single Ended Primary Inductor converter) topology with PV module and MPPT controller is shown in fig5 and it is proposed the converter is operated in Continuous Current Mode (CCM) [2]. The inductance and capacitance values are designed from [10]. This converter has two inductors and two capacitors. The capacitor C1 provides the isolation between input and output. The SEPIC converter exchanges energy between the capacitors and inductors in order to convert the voltage from one level to another. The amount of energy exchanged is controlled by switch, which is typically a transistor such as a MOSFET. L1 is the input inductance, L2 is the output inductance, C1 is the energy transfer capacitor, C2 is the output capacitor, V_{in} is the input voltage, V_o is the output voltage, V_{C1} is the voltage across capacitor C1, I_{L1} is the current through L1 and I_{L2} is the current through L2.

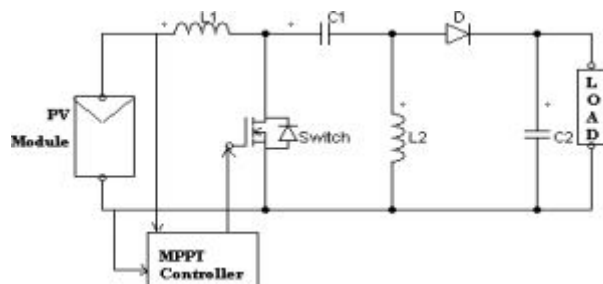
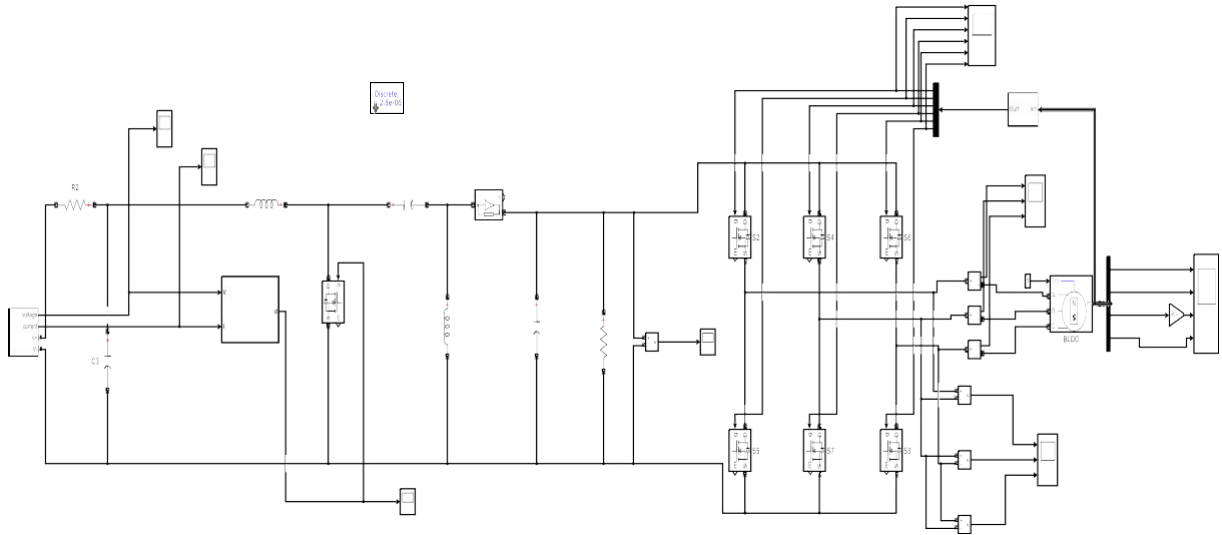


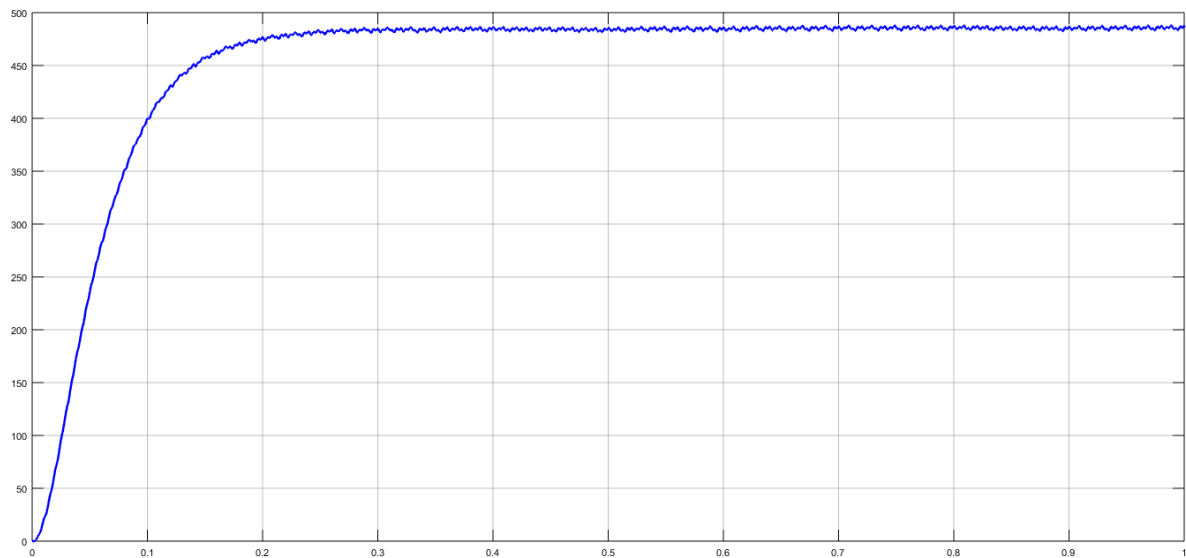
Fig. 5 SEPIC converter topology

SIMULATION OUTPUTS

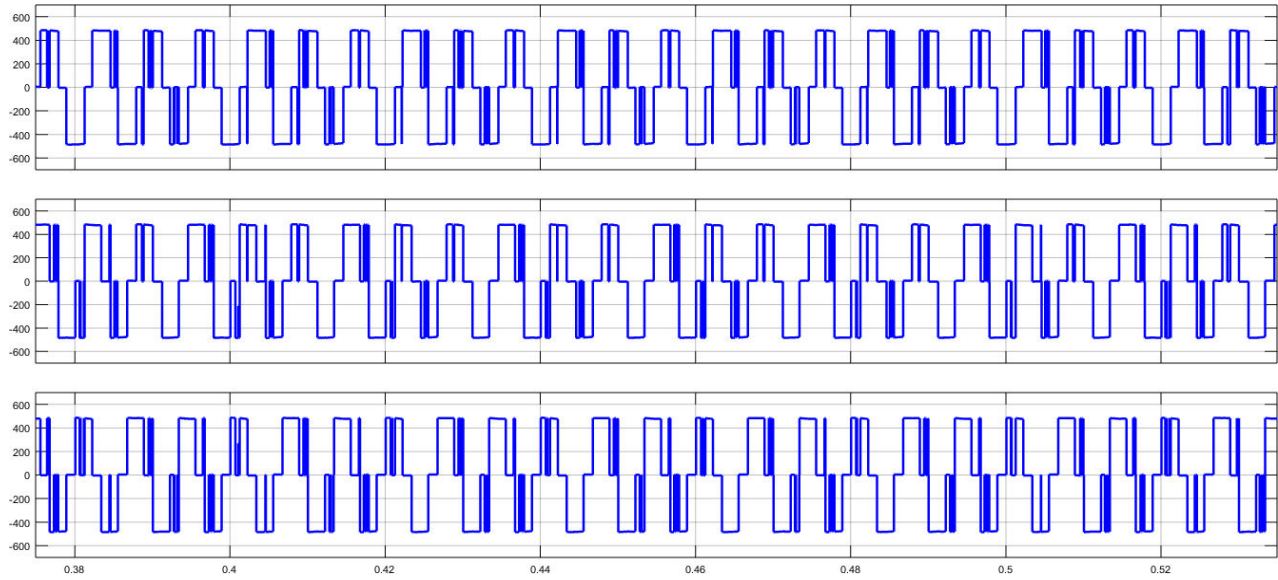
Conventional simulation circuit



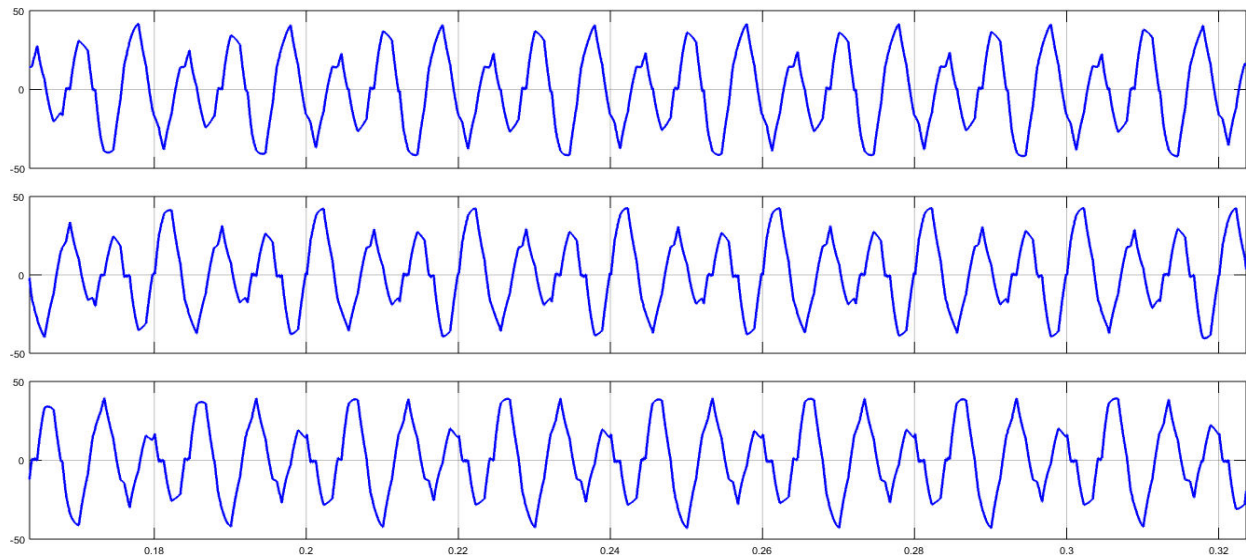
DC Voltage



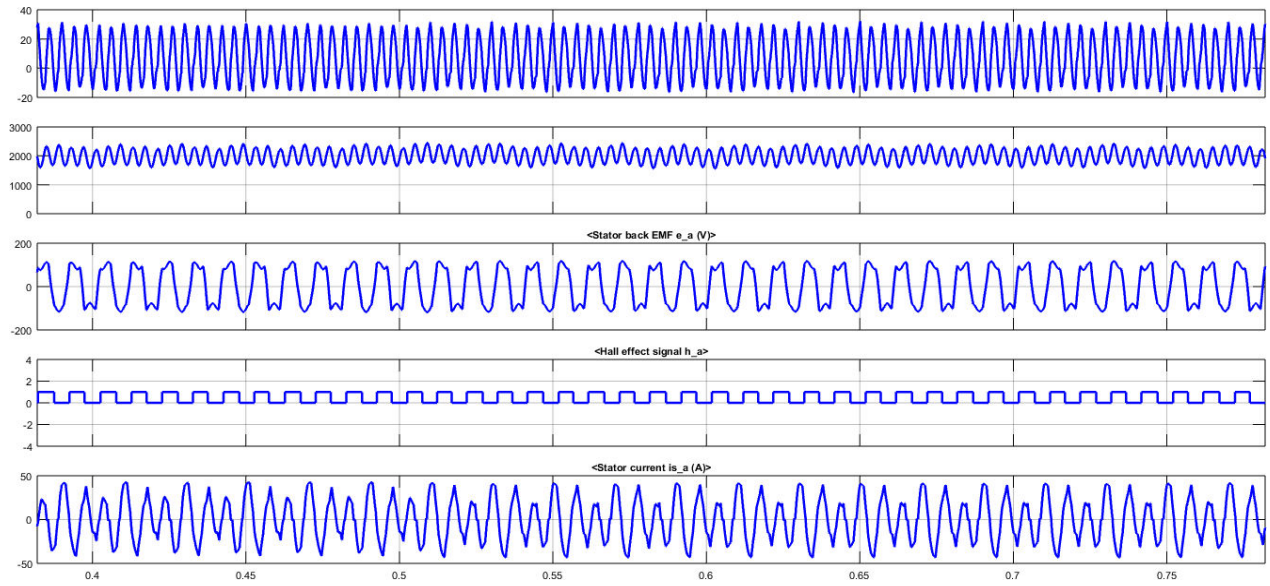
Phase Voltage



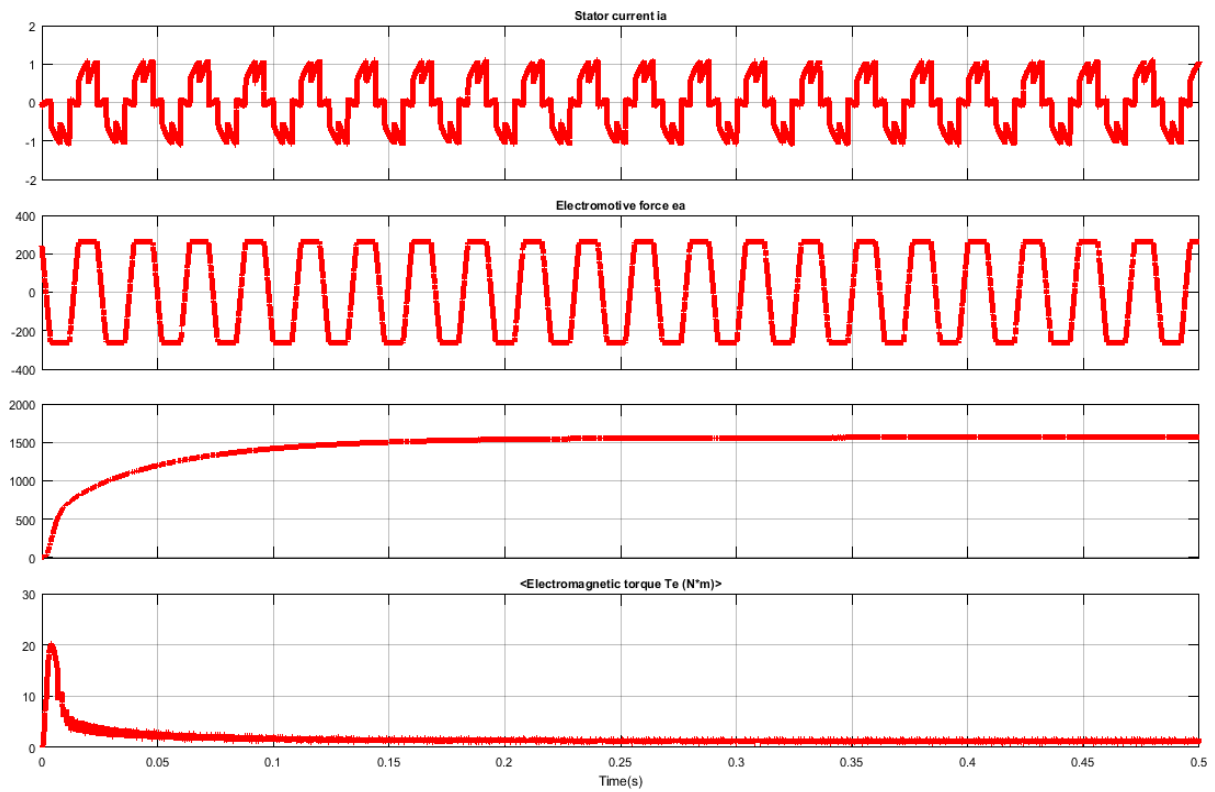
Phase Current



Motor Output



SEPIC converter output:



REFERENCE:

- [1] M. Baszynski, and S. Pirog, "A Novel Speed Measurement Method for a High-Speed BLDC Motor Based on the Signals From the Rotor Position Sensor," *IEEE Transactions on Industrial Informatics*, vol. 10, no. 1, pp. 84-91, 2014.
- [2] V. Bist, and B. Singh, "PFC Cuk Converter-Fed BLDC Motor Drive," *IEEE Transactions on Power Electronics*, vol. 30, no. 2, pp. 871-887, 2015.
- [3] S. Chen, G. Liu, S. Zheng, "Sensorless control of BLDCM drive for a High-Speed maglev blower using a low pass filter," *Power Electronics, IEEE Transactions on*, vol. PP, no. 99, pp. 1-1, 2016.
- [4] S. Zheng, B. Han, R. Feng et al., "Vibration Suppression Control for AMB Supported Motor Driveline System Using Synchronous Rotating Frame Transformation," *Industrial Electronics, IEEE Transactions on*, vol. 62, no. 9, pp. 5700-5708, 2015.
- [5] E. Tang, B. Han, and Y. Zhang, "Optimum Compensator Design for the Flexible Rotor in Magnetically Suspended Motor to Pass the First Bending Critical Speed," *IEEE Transactions on Industrial Electronics*, vol. 63, no. 1, pp. 343-354, 2016.
- [6] C. Zwyssig, J. W. Kolar, and S. D. Round, "Megaspeed Drive Systems: Pushing Beyond 1 Million r/min," *Mechatronics, IEEE/ASME Transactions on*, vol. 14, no. 5, pp. 564-574, 2009.
- [7] Y. Choong-Hyuk, H. In-Joong, and K. Myoung-Sam, "A resolver-to-digital conversion method for fast tracking," *Industrial Electronics, IEEE Transactions on*, vol. 39, no. 5, pp. 369-378, 1992.
- [8] A. M. Bazzi, A. Dominguez-Garcia, and P. T. Krein, "Markov Reliability Modeling for Induction Motor Drives Under Field-Oriented Control," *Power Electronics, IEEE Transactions on*, vol. 27, no. 2, pp. 534-546, 2012.
- [9] Y. Anno, S. Seung-Ki, L. Dong-Cheol et al., "Novel Speed and Rotor Position Estimation Strategy Using a Dual Observer for Low-Resolution Position Sensors," *Power Electronics, IEEE Transactions on*, vol. 24, no. 12, pp. 2897-2906, 2009.
- [10] S. Ogasawara, and H. Akagi, "An approach to position sensorless drive for brushless DC motors." In *Proc. Industry Applications Society Annual Meeting*, Oct 1990, pp. 443-447 vol.1.

